photonics

MDPI

Communication

Inverse Saturable Absorption Mechanism in Mode-Locked Fiber Lasers with a Nonlinear Amplifying Loop Mirror

Xiang Zhang [1,2,†], Yong Shen [1,2,†], Xiaokang Tang [1,2], Qu Liu [1,2] and Hongxin Zou [1,2,*]

1 Institute for Quantum Science and Technology, College of Science, National University of Defense Technology, Changsha 410073, China
2 Hunan Key Laboratory of Mechanism and Technology of Quantum Information, Changsha 410073, China
* Correspondence: hxzou@nudt.edu.cn
† These authors contributed equally to this work.

Abstract: From the perspective of the differential phase delay experienced by the two counterpropagating optical fields, the self-starting of the mode-locked fiber laser with a non-linear amplifying loop mirror (NALM) is theoretically studied. Although it is generally believed that NALM shows a saturable absorption effect on both continuous wave (CW) light and pulses, we find a counter-intuitive fact that cross-phase modulation (XPM) leads to opposite signs of differential non-linear phase shifts (NPSs) in these two cases, resulting in inverse saturable absorption (ISA) during the pulse formation process. The ISA is not helpful for the self-starting of laser mode-locking and can be alleviated by introducing a non-reciprocal phase shifter into the fiber loop. These results are helpful for optimizing the design of NALM and lowering the self-starting threshold of the high-repetition-rate mode-locked fiber laser.

Keywords: saturable absorption; non-linear phase shift; mode-locked fiber laser

check for updates

Citation: Zhang, X.; Shen, Y.; Tang X.; Liu Q.; Zou, H. Inverse Saturable Absorption Mechanism in Mode-Locked Fiber Lasers with a Nonlinear Amplifying Loop Mirror. *Photonics* **2023**, *10*, 261. https://doi.org/10.3390/photonics10030261

Received: 2 February 2023
Revised: 27 February 2023
Accepted: 27 February 2023
Published: 1 March 2023

1. Introduction

Due to their low cost, high stability, and compactness, mode-locked fiber lasers have been widely studied and enabled various applications in recent years. The NALM [1], as a combination of an optical switch non-linear optical loop mirror (NOLM) [2] and a fiber amplifier, is often used as the artificial saturable absorber to achieve mode-locking in fiber lasers [3–5]. In addition, a loss is introduced into the NOLM to make a new asymmetric fiber loop referred to as non-linear absorbing loop mirror (NAbLM) [6–8]. The NOLM and NALM are originally proposed as optical switches, and many optimization methods have been proposed to improve the asymmetry of the fiber loops to facilitate the optical switching function, such as adding absorption loss [7,9,10] or output loss [6,11], making loop dispersion imbalance [12–15], using unbalance splitter [16–19], incorporation of a non-linear element [20–23], introducing a non-reciprocal phase bias [22–24], and using fiber birefringence [2,25–28]. In the last 10 years, these methods have also been used to improve the performance of mode-locked fiber lasers with optical loop mirror.

As far as we know, the state of the art mode-locked erbium-doped fiber lasers with a NALM still have a low repetition rate. For the non-polarization-maintaining scheme, the highest is 257 MHz [29]. For the polarization-maintaining scheme, the highest is 250 MHz [30]. The main limiting factors are the low erbium-doping concentration of the gain fiber, the limited fiber loop length, and the resulting low gain. In addition, the optimization methods mentioned above are not always helpful for the self-starting of high repetition rate mode-locked lasers. It is necessary to find a more effective method from the saturable absorption mechanism of optical loop mirror.

The self-starting of the mode-locking is closely related to the differential NPS accumulation of the two counterpropagating beams in the NALM. There have been many theoretical and experimental studies on self-starting, and their research methods can be roughly divided into three categories. The first is to understand the self-starting through discussing the transmissivity of continuous light and pulsed light separately [13,31,32]. The second is based on the self-starting dynamic model with the assumption that the laser operates instantly in the pulse regime with an equivalent saturable absorber when the modulation for continuous wave is unstable [33,34]. The last is to discuss phenomenologically [35]. For the optical-switch NALM and NOLM, many researchers have found that the XPM effect related to the energy distribution and encounter of lights in fiber loop affects the performance of these two switches [9,10,36,37] and even inverts the switch function [26]. While for the mode-locked fiber laser with a NALM or NOLM, the self-starting of mode-locking is closely related to the differential NPS. Thus, the XPM effect definitely makes a contribution to pulse formation and self-starting in the mode-locked fiber lasers, which has not been thoroughly studied yet.

In order to overcome the difficulties of increasing the repetition rate and analyze the influence of XPM on self-starting of mode-locking, we calculate the power distributions of two counterpropagating beams in the NALM and the differential NPS accumulations. Unlike the three research methods mentioned above, our analysis is carried out from the perspective of NPS accumulation. We find a difference between the differential NPSs for the CW light and the pulses in the fiber loop, which makes the NOLM or NALM show an ISA mechanism during the pulse formation. The ISA has been extensively studied in the real saturable absorber [38–42], but not in the artificial saturable absorber. The ISA in the NOLM or NALM could be used to explain the experimental phenomena that the mode-locking of laser can be actively started by tapping fiber, fine-tuning light polarization, or other disturbances.

2. Theoretical Calculation of EDFA and NPS

Because we only consider the steady states at the beginning and end of laser, the beam propagation in the erbium doped fiber amplifier (EDFA) of a NALM is obtained by employing the Giles model [43]. The Giles model describes an active fiber as a two-level system using four spectroscopic parameters, including the absorption spectrum α, the gain spectrum g^*, the saturation parameter ζ, and the linear loss l. The optical power of the k-th beam $P_k(z)$ at position z and the ratio of ions in the excited state $\bar{N}_2/\bar{N}_1$ are described as

$$\frac{dP_k}{dz} = u_k(\alpha_k + g_k^*)\frac{\bar{N}_2}{\bar{N}_t}P_k(z) + 2u_k g_k^* \frac{\bar{N}_2}{\bar{N}_t} h\nu_k \Delta\nu_k - u_k(\alpha_k + l_k)P_k, \tag{1}$$

$$\frac{\bar{N}_2}{\bar{N}_t} = \frac{\Sigma_k \frac{P_k(z)\alpha_k}{h\nu_k\zeta}}{1 + \Sigma_k \frac{P_k(z)(\alpha_k + g_k^*)}{h\nu_k\zeta}}, \tag{2}$$

where $h\nu_k$ is the photon energy, $\Delta\nu$ is the frequency bandwidth of the beam, $u_k = \pm 1$ denotes the propagation direction of the beam.

The non-linear effects considered in our model include self-phase modulation (SPM) and XPM. SPM refers to the self-induced phase shift experienced by an optical field E during its propagation in optical fibers, whose magnitude is

$$\phi_{\mathrm{SPM}} = \bar{n}_2 k_0 \int_0^L |E(z)|^2 dz = \gamma \int_0^L P(z) dz, \tag{3}$$

where $\bar{n}_2$ is the non-linear-index coefficient, and $\gamma = 2\pi n_2/(\lambda A_{\mathrm{eff}})$ is the non-linear coefficient of fiber. In our system, γ_1 of the passive fiber is 1.367 $\mathrm{W}^{-1}/\mathrm{km}$, and γ_2 of the erbium-doped fiber is 2.134 $\mathrm{W}^{-1}/\mathrm{km}$. XPM refers to the differential NPS of an optical field induced by another field with a different wavelength, propagation direction, or polarization. Since the beams in NALM have the same polarization and counter propagate, the XPM coefficient is equal to 2. Other non-linear effects except for SPM and XPM are not considered in the following calculations.

The configuration of NALM is shown in Figure 1. Since the gain fiber takes up a large portion of the loop, the influence of optical power distribution in the gain fiber on the differential NPS accumulation needs to be considered. Before pulse formation, the light in the cavity is a continuous wave with low power. Thus, we regard the initial light as CW light with amplitude A_0. As such an optical signal enters the input port of the NALM, amplitudes of the forward and backward propagating fields are given by

$$A_f(0) = \sqrt{\rho}A_0, \quad A_b(0) = i\sqrt{1-\rho}A_0. \tag{4}$$

After one round trip, both fields acquire a linear phase shift and differential NPSs induced by SPM and XPM [44], and can be written as

$$A'_f = \sqrt{\rho}\sqrt{g_f}A_0 \exp\left(i\phi_0 + i\phi_f\right), \quad A'_b = i\sqrt{1-\rho}\sqrt{g_b}A_0 \exp\left(i\phi_0 + i\phi_b\right), \tag{5}$$

where ϕ_0 is the linear phase shift, g_f and g_b are the gain factors of the forward and backward fields, respectively. Since the fiber is short, the fiber loss is neglected in the calculation.

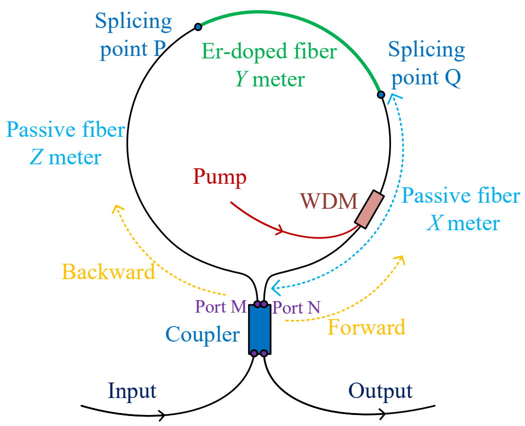

Figure 1. The configuration of NALM. The length of passive fiber from port N to splicing point Q is X meter. The length of Er-doped fiber is Y meter. The length of passive fiber from port M to splicing point P is Z meter. The counterclockwise beam and the clockwise beam are named forward beam and backward beam, respectively. Their optical intensity ratio is $\rho : (1-\rho)$.

As the two beams are output from the M and N ports, respectively, and counter propagate in fiber, the SPM phase shifts start to be generated. Then they meet in the gain fiber and indirectly interact with each other through the medium to generate the XPM phase shifts. Thus, the NPSs of the forward and the backward beams can be divided into four parts and expressed by SPM and XPM terms as

$$\begin{aligned}\phi_f =& \gamma_1\rho|A_0|^2X + \gamma_2\int_X^{\frac{X+Y+Z}{2}} \left|A_f(z)\right|^2 dz + \gamma_2\int_{\frac{X+Y+Z}{2}}^{\frac{3X+Y+Z}{2}} \left|A_f(z)\right|^2 + 2|A_b(z)|^2 dz \\ &+ \gamma_1\left[\rho g_f + 2(1-\rho)\right]|A_0|^2Z,\end{aligned} \tag{6}$$

$$\begin{aligned}\phi_b =& \gamma_1[(1-\rho)g_b + 2\rho]|A_0|^2X + \gamma_2\int_X^{\frac{X+Y+Z}{2}} 2\left|A_f(z)\right|^2 + |A_b(z)|^2 dz \\ &+ \gamma_2\int_{\frac{X+Y+Z}{2}}^{\frac{3X+Y+Z}{2}} |A_b(z)|^2 dz + \gamma_1(1-\rho)|A_0|^2Z,\end{aligned} \tag{7}$$

and the differential NPS is

$$\begin{aligned}\phi_f - \phi_b =& \gamma_1 |A_0|^2 X(\rho g_b - g_b - \rho) - \gamma_2 \int_X^{\frac{X+Y+Z}{2}} \left|A_f(z)\right|^2 + |A_b(z)|^2 dz \\ &+ \gamma_2 \int_{\frac{X+Y+Z}{2}}^{\frac{3X+Y+Z}{2}} \left|A_f(z)\right|^2 + |A_b(z)|^2 dz + \gamma_1 |A_0|^2 Z\left(\rho g_f - \rho + 1\right),\end{aligned} \tag{8}$$

where we assume $X < (X+Y+Z)/2 < X+Y$, z is the distance from the light wavefront to port M, $A_f(z)$ and $A_b(z)$ are the amplitudes of forward and backward electric field of the light beam at z, respectively. Before self-starting of the mode-locked laser, the light in the cavity is CW, whose differential NPS can be obtained with Equation (8). Since only two counterpropagating pulses exhibit in the cavity when the laser modes are locked, the XPM phase shift that contributes to differential NPS is only generated where the pulses meet and can be neglected. Therefore, the differential NPS of the pulsed light is only related to SPM and can be expressed as

$$\begin{aligned}\phi_f - \phi_b =& \gamma_1 |A_0|^2 \left[\rho g_f + \rho - 1 + X\left(1 - g_b + \rho g_b - \rho g_f\right)\right] \\ &+ \gamma_2 \int_X^{\frac{3X+Y+Z}{2}} |A_f(z)|^2 - |A_b(z)|^2 dz.\end{aligned} \tag{9}$$

3. Results and Discussion

3.1. Inverse Saturable Absorption Mechanism in NALM

We assume that the peak power of the pulsed light is equal to the power of the CW light. Based on Equations (8) and (9), we can obtain the NPSs of the two beams in the NALM, which are shown in Figure 2a,b, respectively. It is evident that the difference between phase delay ϕ_f and phase delay ϕ_b of CW light decreases to zero and becomes positive as a result of XPM after the two beams meet, whereas the differential NPS of pulsed light increases further. In the NALM mode-locked fiber laser, as the power of the light in the cavity increases, the light evolves from CW to pulses, and the differential-NPS-sign transition can occur during the self-starting of mode-locking.

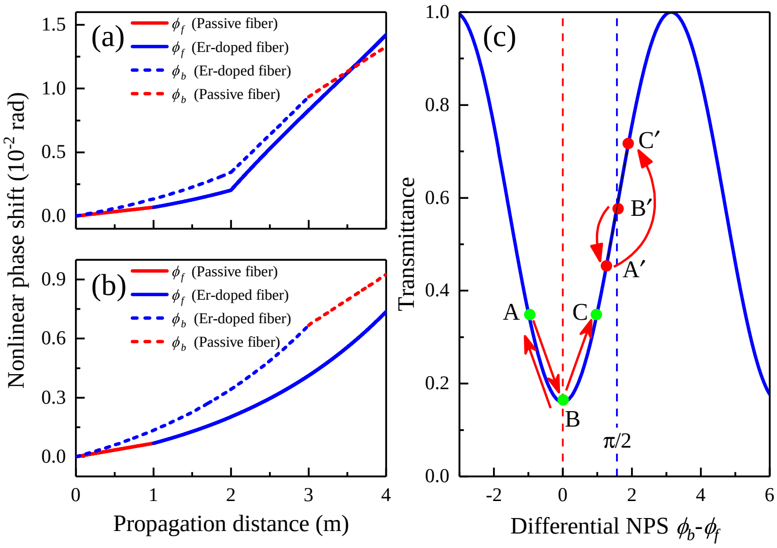

Figure 2. (**a**) NPS of the CW light in NALM. (**b**) NPS of the pulsed light in NALM. (**c**) The NOLM transmittance as functions of the differential NPS. For the NALM, the splitting ratio is 0.5, the passive fiber length $X = 1$ m, $Z = 0$ and the Er-doped fiber length $Y = 3$ m. Point B is at $\phi_f - \phi_b = 0$, Point B′ is at $\phi_f - \phi_b = \pi/2$. Points A and A′ are differential NPS inflection points, and point A′ is not on the left side of point B. Points C and C′ are any points of the uphill curve, to the right of points B and B′, respectively.

We discuss the influence of this differential-NPS-sign transition on the saturable absorption effect of the NALM and self-starting of mode locking based on the transmittance curve of NOLM given in Figure 2c. Here, we choose to discuss NOLM instead of NALM for convenience. In the process of optical signal changing from CW to pulses, point B at $\phi_f - \phi_b = 0$ has two roles. One is the point where the pump is turned on, and the other is the point where the sign of the differential NPS changes. When the pump is turned on, the optical signal is continuous, and the round-trip differential NPS increases along the trace B $\rightarrow$ A, which is manifested as positive feedback with less loss for the stronger light and more loss for the weaker light. Therefore, it is the saturable absorption effect that favors the formation of pulses. When the light gradually evolves from CW to pulses, the differential NPS moves along A $\rightarrow$ B $\rightarrow$ C, as depicted in Figure 2c. As the peak-to-average power ratio of the pulse gradually increases, the SPM effect dominates over the XPM effect, resulting in a change in the sign of the differential NPS. In the A $\rightarrow$ B process, the fiber loop shows negative feedback, i.e., the stronger the light, the greater the loss. Therefore, the so-called ISA effect merges, which is not helpful to the formation of the pulses. If the differential NPS of two optical beams cannot exceed this negative feedback range, the mode-locking can not be achieved. In the B $\rightarrow$ C process, the fiber loop shows positive feedback. Although the B $\rightarrow$ A and B $\rightarrow$ C processes are in opposite traces on the horizontal axis, they both show saturable absorption.

Since the slope at point B is zero, the transmittance differences for low-intensity lights around point B are close to zero and do not offer any intensity-dependent transmittance. In order to weaken the negative impacts of the process A $\rightarrow$ B and point B on differential NPS accumulation, a simple method is adding a $\pi/2$ phase shifter to the fiber loop, so as to move points A, B, and C to points A$'$, B$'$, and C$'$, respectively. As a result, both the initial transmittance of the light and the slope of the initial point will increase. When the phase shifter is inserted, the trace of the differential NPS is still B$'$ $\rightarrow$ A$'$ $\rightarrow$ B$'$ $\rightarrow$ C$'$, but the feedback type has changed. In the B$'$ $\rightarrow$ A$'$ process, the fiber loop shows negative feedback. In the A$'$ $\rightarrow$ B$'$ $\rightarrow$ C$'$ process, the fiber loop shows positive feedback. The phase shifter prevents the light in the fiber loop from forming pulses in the opposite traces, such as B $\rightarrow$ A and B $\rightarrow$ C. It reduces the difficulty of turning around at point A and helps to accumulate the differential NPS in the correct trace when the sign change of differential NPS occurs.

After self-starting of mode locking, the pump power can be gradually reduced to a low level, while mode-locking still keeps. The mode-locking stability should be related to the fact that the pulsed light in the NALM does not experience the A $\rightarrow$ B negative feedback region. When the pump power is too low to support mode locking, the light will change from pulsed light to continuous light, and the output optical power will suddenly increase [45]. This can be attributed to the sign change of differential NPS mentioned above.

In addition to increasing the power pump and introducing a phase shifter, the mode locking can also be achieved by adding a polarization controller on the fiber loop, tapping the fiber, slightly rotating the wave plate in the phase shifter, using an intra-cavity amplitude modulator to initiate the pulses [46,47], or putting a moving mirror at the output port [48]. In addition, it has been verified in our experiment that mode locking of a figure-9 fiber laser with the configuration in Ref. [30] can be achieved by placing a moving aluminum alloy plate or a piece of paper at one of the two PBS output ports after the pump light is injected. While these methods can reduce the mode-locking threshold, one disadvantage is that after actively starting the mode-locking, the mode-locking cannot self-start after restarting the laser. Another disadvantage is that the same characteristics of the output pulse are also difficult to reproduce. For example, the pulse width may vary widely. The main principle of actively start mode-locking is that these methods suddenly change the phase of the laser beam, which is equivalent to directly inputting high-power optical signal to skip the negative feedback region of NALM or NOLM, rather than gradually cyclically amplifying the small optical signal in the cavity to evolve a stable phase shift. Moreover, in the experiment, we found that placing a static aluminum alloy plate or a piece of static paper at one of the two PBS output ports before the pump light is injected can make the self-starting threshold of the laser's mode-locking higher or prevent self-starting.

3.2. Different Effects of Splitting Ratio and Optical Attenuator on NOLM

Considering the phase shift $\pi/2$ brought by the coupler, the round-trip transmittance of NOLM is

$$T \equiv \frac{|A_t|^2}{|A_0|^2} = 1 - 2\rho(1-\rho)\left[1 + \cos\left(\phi_f - \phi_b\right)\right]. \quad (10)$$

Here, the differential NPS is

$$\phi_f - \phi_b = (1-2\rho)\gamma|A_0|^2 L. \quad (11)$$

When loss $1-\alpha$ is added to the coupler's forward light output port N, the transmittance becomes

$$T_{\mathrm{N}} \equiv \frac{|A_t|^2}{\alpha|A_0|^2} = 1 - 2\rho(1-\rho)\left\{1 + \cos\left[(1-\rho-\alpha\rho)\gamma|A_0|^2 L\right]\right\}, \quad (12)$$

where the differential NPS is $(1-\rho-\alpha\rho)\gamma|A_0|^2 L$, and α is the optical transmittance of the loss. If the light intensity of the forward light is greater than that of the backward light ($\rho > 0.5$), the absolute value of the differential NPS in Equation (12) is always smaller than that in Equation (11), that is, the loss is not helpful to the differential NPS accumulation. If $\rho < 0.5$, the loss is helpful, and it can increase the differential NPS and help lower self-starting threshold of the mode-locked laser with this NOLM. When the loss $1-\alpha$ is added at the intermediate position of the fiber between port M and port N, the transmittance becomes

$$T_{\mathrm{mid}} \equiv \frac{|A_t|^2}{\alpha|A_0|^2} = 1 - 2\rho(1-\rho)\left\{1 + \cos\left[(\alpha+1)\left(\frac{1}{2}-\rho\right)\gamma|A_0|^2 L\right]\right\}, \quad (13)$$

where the differential NPS is $(\alpha+1)(1/2-\rho)\gamma|A_0|^2 L$, which is always smaller than that of Equation (11).

Although both the splitting ratio and the optical attenuator in the fiber loop can change the intensity ratio of the two counterpropagating beams, they have different effects on the round-trip transmittance of the NOLM. Figure 3 shows the influence of splitting ratio and optical attenuator on the transmittance of NOLM. By comparing the NPS parameters corresponding to the first maximum value of the three curves T_{a}, T_{b}, and T_{c}, it can be seen that the closer the splitting ratio ρ is to 0.5, the larger the NPS parameter is required to achieve the maximum transmittance. In addition, the minimum transmittance of the curve T_{c} is smaller than that of the curves T_{a} and T_{c}, that is, the modulation depth of the NOLM corresponding to curve T_{c} is the largest.

Under the same splitting ratio as curve T_{c}, the curves T_{N} and T_{mid} in Figure 3 are obtained after introducing a 10% loss into the fiber loop. It can be seen that their highest points are located on either side of the highest point of curve T_{c}. Unlike the case with different splitting ratios, the minimum transmissivities of curves T_{N} and T_{mid} are the same as that of curve T_{c}, and the loss only changes the position of the maximum transmittance. To compare the different effects of splitting ratio and optical attenuator on NOLM more intuitively, we can consider the curves T_{N} and T_{b}. The splitting ratio of curve T_{b} is set according to

$$\rho' = \frac{\rho_c(1-\alpha)}{1-\rho_c} \quad (14)$$

where ρ_c is the beam splitting ratio of the curve T_{c}, $1-\alpha$ is the loss, and the $\alpha = 0.9$. Thus, the light intensities of two beams with a ratio of ρ' are close to that of the two beams with a ratio of ρ_c and a loss of $1-\alpha$ are added at the point N. It is clear that the curve T_{N} is only slightly shifted to the right relative to the curve T_b, while the minimum transmittance is smaller than that of the curve T_b.

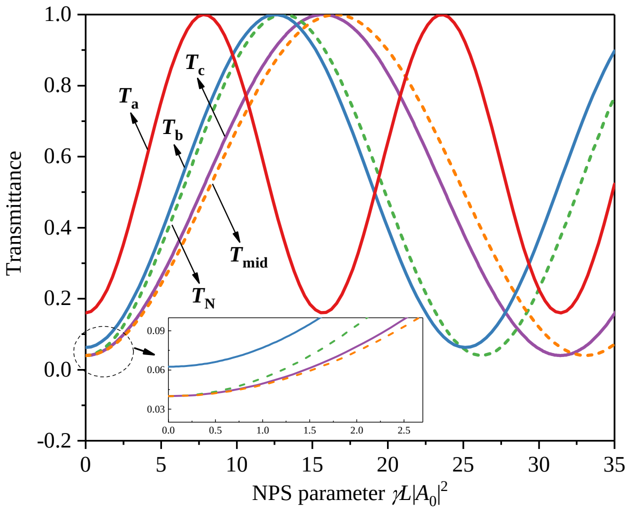

Figure 3. Variation of NOLM transmittance with NPS parameter $\gamma L|A_0|^2$. The L is the length of the fiber loop. The five transmittance curves are plotted at different splitting ratios (ρ) and losses ($1-\alpha$), where T_a: $\rho = 0.3$, T_b: $\rho = 0.375$, T_c: $\rho = 0.4$, T_N: $\rho = 0.4, \alpha = 0.9$ and loss is added at port N, T_{mid}: $\rho = 0.4, \alpha = 0.9$ and loss is added at the midpoint of the fiber between port N and port M.

We know that the closer ρ is to 0.5, the greater the modulation depth of the NOLM. However, when $\rho = 0.5$, NOLM does not show a saturation absorption effect. If the optical attenuator is added in NOLM, this problem can be avoided and the maximum modulation depth can be obtained. The optical attenuator here acts similarly to the gain fiber in NALM [8], but has no drawbacks: the gain of fiber is distributed along a line rather than at a point and the differential NPS between the two counterpropagating beams is not obvious when the gain fiber accounts for a large proportion of the fiber loop. In addition, before the two counterpropagating beams meet and interfere in the coupler, this loss can also effectively reduce the optical power difference introduced by the gain fiber and the coupler to make the NALM have a higher modulation depth.

A figure-9 fiber laser is one of the most popular mode-locked lasers at present. It has some characteristics different from those mentioned above. For the figure-9 fiber laser with a coupler, according to Equation (10), its transmittance is

$$T' = 1 - T. \tag{15}$$

Therefore, the transmittance curves are the reversal of the curves in Figure 3, and a phase shifter must be injected in the fiber loop so that the figure-9 configuration can show saturable absorption effect at the initial stage. The maximum transmittance is not equal to 1, and the minimum transmittance is zero. It can be seen that when the beam splitting ratio is far away from 0.5, the maximum transmittance will be reduced, and the large difference between the two interfering beams may raise the noise level intracavity [35,49], while controlling the energy ratio of the two beams through optical attenuator will avoid this situation. However, for the figure-9 fiber laser with a PBS, the maximum and minimum transmittance will not change [50].

In practice, once the laser is built, it is often difficult to adjust the coupler's splitting ratio, while the loss can be continuously adjusted and compensated by increasing the gain in the cavity. The loss can also be induced via the output loss, where a suitable beam splitter can be freely introduced in the loop to improve loop asymmetry. The output loss of the fiber loop can be used for other applications, such as signal monitor and amplifier seed. Additionally, it is found in an experiment that the quality of the pulse at different output ports is different [51,52], and the quality of the pulse output inside the loop is higher than that outside the loop.

4. Conclusions

We study the self-starting of the mode-locked fiber laser with a NALM by calculating the phase shift evolution in the fiber loop. We review the experiments of others in this paper to avoid repeating them to increase space. By comparing the round-trip differential NPS signs of the CW light and the pulses, we find that the NALM can behave as an inverse saturable absorber during the pulse formation process, which is not helpful for pulse formation and mode-locking self-starting. The impact of ISA can be alleviated by introducing a non-reciprocal phase shifter into the fiber loop and shifting the ISA region on the transmittance curve. In addition, we analyze the different effects of splitting ratio and optical attenuator on NOLM. It is found that although both the splitting ratio and the optical attenuator can change the intensity ratio of the two interfering beams, they have different effects on the round-trip transmittance curve of the optical loop mirror. The increase in beam splitting ratio can reduce the amplitude of transmittance curve and increase the slope of curve, while the optical attenuator does not change the amplitude of curve. At present, for the mode-locked fiber laser with a NALM, how to reduce the difficulty of manufacturing the high-repetition-rate fiber laser and how to lower the self-starting threshold are urgent problems to be solved. The discussions about the ISA mechanism and the different effects of splitting ratio and optical attenuator are of potential help in these areas.

Author Contributions: Conceptualization, X.Z. and Y.S.; methodology, X.Z.; software, X.Z.; validation, X.Z., X.T. and Q.L.; formal analysis, X.Z.; investigation, X.Z.; resources, X.Z.; data curation, X.Z.; writing—original draft preparation, X.Z. and Y.S.; writing—review and editing, X.Z. and Y.S.; visualization, X.Z.; supervision, Y.S.; project administration, Y.S. and H.Z.; funding acquisition, Y.S. and H.Z. All authors have read and agreed to the published version of the manuscript.

Funding: This research was funded by National Natural Science Foundation of China (62105368 and 62275268).

Institutional Review Board Statement: Not applicable.

Informed Consent Statement: Not applicable.

Data Availability Statement: Not applicable.

Acknowledgments: We would like to thank Ke Yin for the instruction on our work, Guochao Wang for the discussions about mode-locked fiber laser, and Joona Rissanen for the rate equation simulation library PyFiberAmp at https://github.com/Jomiri/pyfiberamp (accessed on 22 October 2022).

Conflicts of Interest: The authors declare no conflict of interest.

Abbreviations

The following abbreviations are used in this manuscript:

CW	continuous wave
NALM	non-linear amplifying loop mirror
XPM	cross-phase modulation
NPS	non-linear phase shift
ISA	inverse saturable absorption
NOLM	non-linear optical loop mirror
NAbLM	non-linear absorbing loop mirror
EDFA	erbium doped fiber amplifier
SPM	self-phase modulation

References

1. Fermann, M.E.; Haberl, F.; Hofer, M.; Hochreiter, H. Nonlinear Amplifying Loop Mirror. *Opt. Lett.* **1990**, *15*, 752. [CrossRef] [PubMed]
2. Doran, N.J.; Wood, D. Nonlinear-Optical Loop Mirror. *Opt. Lett.* **1988**, *13*, 56. [CrossRef] [PubMed]
3. Duling, I. Subpicosecond All-Fibre Erbium Laser. *Electron. Lett.* **1991**, *27*, 544. [CrossRef]
4. Fermann, M.E.; Hofer, M.; Haberl, F.; Schmidt, A.J.; Turi, L. Additive-Pulse-Compression Mode Locking of a Neodymium Fiber Laser. *Opt. Lett.* **1991**, *16*, 244–246. [CrossRef]
5. Richardson, D.; Laming, R.; Payne, D.; Matsas, V.; Phillips, M. Selfstarting, Passively Modelocked Erbium Fibre Ring Laser Based on the Amplifying Sagnac Switch. *Electron. Lett.* **1991**, *27*, 542. [CrossRef]
6. Bulushev, A.G.; Dianov, E.M.; Okhotnikov, O.G. Self-Starting Mode-Locked Laser with a Nonlinear Ring Resonator. *Opt. Lett.* **1991**, *16*, 88–90. [CrossRef]
7. Seong, N.H.; Kim, D.Y.; Veetil, S.P. Mode-Locked Fiber Laser Based on an Attenuation-Imbalanced Nonlinear Optical Loop Mirror. *Opt. Commun.* **2007**, *280*, 438–442. [CrossRef]
8. Zhao, J.; Zhou, J.; Jiang, Y.; Li, L.; Shen, D.; Komarov, A.; Su, L.; Tang, D.; Klimczak, M.; Zhao, L. Nonlinear Absorbing-Loop Mirror in a Holmium-Doped Fiber Laser. *J. Light. Technol.* **2020**, *38*, 6069–6075. [CrossRef]
9. Bogoni, A.; Scaffardi, M.; Ghelfi, P.; Poti, L. Nonlinear Optical Loop Mirrors: Investigation Solution and Experimental Validation for Undesirable Counterpropagating Effects in All-Optical Signal Processing. *IEEE J. Sel. Top. Quantum Electron.* **2004**, *10*, 1115–1123. [CrossRef]
10. Pitois, S. Influence of Cross-Phase Modulation in SPM-Based Nonlinear Optical Loop Mirror. *Opt. Commun.* **2005**, *253*, 332–337. [CrossRef]
11. Ai, F.; Cao, Z.; Zhang, X.; Zhang, C.; Zhang, B.; Yu, B. Passively Mode-Locked Fiber Laser with Kilohertz Magnitude Repetition Rate and Tunable Pulse Width. *Opt. Laser Technol.* **2011**, *43*, 501–505. [CrossRef]
12. Steele, A. Pulse Compression by an Optical Fibre Loop Mirror Constructed from Two Different Fibres. *Electron. Lett.* **1993**, *29*, 1972. [CrossRef]
13. Wong, W.S.; Namiki, S.; Margalit, M.; Haus, H.A.; Ippen, E.P. Self-Switching of Optical Pulses in Dispersion-Imbalanced Nonlinear Loop Mirrors. *Opt. Lett.* **1997**, *22*, 1150. [CrossRef] [PubMed]
14. Matsumoto, M.; Ohishi, T. Dispersion-Imbalanced Nonlinear Optical Loop Mirror with Lumped Dispersive Elements. *Electron. Lett.* **1998**, *34*, 1140. [CrossRef]
15. Yongkui, D.; Yongqiang, W.; Zhiyong, L.; Li, T.; Shichen, L. Pulse Amplitude Equalization in a Harmonically Modelocked Fiber Laser Using a Dispersion Imbalanced Non-Linear Loop Mirror. *Opt. Commun.* **2003**, *225*, 363–369. [CrossRef]
16. Mortimore, D. Fiber Loop Reflectors. *J. Light. Technol.* **1988**, *6*, 1217–1224. [CrossRef]
17. Steele, A.L.; Hemingway, J.P. Nonlinear Optical Loop Mirror Constructed from Dispersion Decreasing Fibre. *Opt. Commun.* **1996**, *123*, 487–491. [CrossRef]
18. Shah, D.D.; Ravikanth, J.; Vijaya, R. Optimization of Peak Transmittivity in a Non-Linear Fiber Loop Mirror—an Accurate Analysis. *Opt. Commun.* **2001**, *197*, 301–308. [CrossRef]
19. Meissner, M.; Rösch, M.; Schmauss, B.; Leuchs, G. Optimum Splitting Ratio for Amplifier Noise Reduction by an Asymmetric Nonlinear Optical Loop Mirror. *Appl. Phys. B* **2005**, *80*, 489–495. [CrossRef]
20. Kane, M.G.; Glesk, I.; Sokoloff, J.P.; Prucnal, P.R. Asymmetric Optical Loop Mirror: Analysis of an All-Optical Switch. *Appl. Opt.* **1994**, *33*, 6833. [CrossRef]
21. Sponsel, K.; Cvecek, K.; Stephan, C.; Onishchukov, G.; Schmauss, B.; Leuchs, G. Optimization of a Nonlinear Amplifying Loop Mirror for Amplitude Regeneration in Phase-Shift-Keyed Transmission. *IEEE Photon. Technol. Lett.* **2007**, *19*, 1858–1860. [CrossRef]
22. Hierold, M.; Roethlingshoefer, T.; Sponsel, K.; Onishchukov, G.; Schmauss, B.; Leuchs, G. Multilevel Phase-Preserving Amplitude Regeneration Using a Single Nonlinear Amplifying Loop Mirror. *IEEE Photon. Technol. Lett.* **2011**, *23*, 1007–1009. [CrossRef]
23. Zhang, S.; Wu, B.; Wen, F. Phase-Preserving NALM Regenerator with Lower Input Power by Optimizing the Nonreciprocal Phase Shifter. *Appl. Opt.* **2021**, *60*, 492. [CrossRef] [PubMed]
24. Hong L.; Donald, D.; Sorin, W. Optimizing Polarization States in a Figure-8 Laser Using a Nonreciprocal Phase Shifter. *J. Light. Technol.* **1994**, *12*, 1121–1128. [CrossRef]
25. Moores, J.D.; Bergman, K.; Haus, H.A.; Ippen, E.P. Optical Switching Using Fiber Ring Reflectors. *J. Opt. Soc. Am. B* **1991**, *8*, 594. [CrossRef]
26. Finlayson, N.; Nayar, B.K.; Doran, N.J. Switch Inversion and Polarization Sensitivity of the Nonlinear-Optical Loop Mirror. *Opt. Lett.* **1992**, *17*, 112. [CrossRef]
27. Rhy, H.Y.; Kim, B.Y.; Lee, H.W. Self-Switching with a Nonlinear Birefringent Loop Mirror. *IEEE J. Quantum Electron.* **2000**, *36*, 89–93. [CrossRef]
28. Pottiez, O.; Kuzin, E.A.; Ibarra-Escamilla, B.; Camas-Anzueto, J.T.; Gutiérrez-Zainos, F. Easily Tunable Nonlinear Optical Loop Mirror Based on Polarization Asymmetry. *Opt. Express* **2004**, *12*, 3878. [CrossRef]
29. Gao, W.; Liu, G.; Zhang, Z. 44.6 fs Pulses from a 257 MHz Er:Fiber Laser Mode-Locked by Biased NALM. *Chin. Opt. Lett.* **2018**, *16*, 111401. [CrossRef]

30. Hänsel, W.; Hoogland, H.; Giunta, M.; Schmid, S.; Steinmetz, T.; Doubek, R.; Mayer, P.; Dobner, S.; Cleff, C.; Fischer, M.; et al. All Polarization-Maintaining Fiber Laser Architecture for Robust Femtosecond Pulse Generation. *Appl. Phys. B* **2017**, *123*, 41. [CrossRef]
31. Duling, I.; Chen, C.J.; Wai, P.; Menyuk, C. Operation of a Nonlinear Loop Mirror in a Laser Cavity. *IEEE J. Quantum Electron.* **1994**, *30*, 194–199. [CrossRef]
32. Mayer, A.S.; Grosinger, W.; Fellinger, J.; Winkler, G.; Perner, L.W.; Droste, S.; Salman, S.H.; Li, C.; Heyl, C.M.; Hartl, I.; et al. Flexible All-PM NALM Yb:Fiber Laser Design for Frequency Comb Applications: Operation Regimes and Their Noise Properties. *Opt. Express* **2020**, *28*, 18946. [CrossRef] [PubMed]
33. Chen, C.J.; Wai, P.K.A.; Menyuk, C.R. Self-Starting of Passively Mode-Locked Lasers with Fast Saturable Absorbers. *Opt. Lett.* **1995**, *20*, 350. [CrossRef] [PubMed]
34. Leke, P.A.; Dikandé, A.M. Dynamics of Passively Mode-Locked Lasers with Saturable Absorber and Saturable Nonlinearity. *Appl. Phys. B* **2020**, *126*, 157. [CrossRef]
35. Liao, R.; Song, Y.; Chai, L.; Hu, M. Pulse Dynamics Manipulation by the Phase Bias in a Nonlinear Fiber Amplifying Loop Mirror. *Opt. Express* **2019**, *27*, 14705. [CrossRef] [PubMed]
36. Jinno, M.; Matsumoto, T. Nonlinear Sagnac Interferometer Switch and Its Applications. *IEEE J. Quantum Electron.* **1992**, *28*, 875–882. [CrossRef]
37. Clausen, C.B.; Povlsen, J.H.; Rottwitt, K. Polarization Sensitivity of the Nonlinear Amplifying Loop Mirror. *Opt. Lett.* **1996**, *21*, 1535. [CrossRef]
38. Keller, U. *Ultrafast Lasers: A Comprehensive Introduction to Fundamental Principles with Practical Applications*; Springer Nature Switzerland AG: Cham, Switzerland, 2021.
39. Li, X.; Wang, Y.; Wang, Y.; Zhao, W.; Yu, X.; Sun, Z.; Cheng, X.; Yu, X.; Zhang, Y.; Wang, Q.J. Nonlinear Absorption of SWNT Film and Its Effects to the Operation State of Pulsed Fiber Laser. *Opt. Express* **2014**, *22*, 17227–17235. [CrossRef]
40. Grange, R.; Haiml, M.; Paschotta, R.; Spühler, G.; Krainer, L.; Golling, M.; Ostinelli, O.; Keller, U. New regime of inverse saturable absorption for self-stabilizing passively mode-locked lasers. *Appl. Phys. B* **2005**, *80*, 151–158. [CrossRef]
41. Saraceno, C.J.; Schriber, C.; Mangold, M.; Hoffmann, M.; Heckl, O.H.; Baer, C.R.; Golling, M.; Südmeyer, T.; Keller, U. SESAMs for High-Power Oscillators: Design Guidelines and Damage Thresholds. *IEEE J. Select. Top. Quantum Electron.* **2012**, *18*, 29–41. [CrossRef]
42. Schibli, T.; Thoen, E.; Kärtner, F.; Ippen, E. Suppression of Q-switched mode locking and break-up into multiple pulses by inverse saturable absorption. *Appl. Phys. B* **2000**, *70*, S41–S49. [CrossRef]
43. Giles, C.; Desurvire, E. Modeling Erbium-Doped Fiber Amplifiers. *J. Light. Technol.* **1991**, *9*, 271–283. [CrossRef]
44. Agrawal, G. *Nonlinear Fiber Optics*, 6th ed.; Elsevier Inc.: Cambridge, UK, 2019.
45. Grudinin, A.; Richardson, D.; Payne, D. Energy Quantisation in Figure Eight Fibre Laser. *Electron. Lett.* **1992**, *28*, 67–68. [CrossRef]
46. Nicholson, J.W.; Andrejco, M. A Polarization Maintaining, Dispersion Managed, Femtosecond Figure-Eight Fiber Laser. *Opt. Express* **2006**, *14*, 8160. [CrossRef]
47. Baumann, E.; Giorgetta, F.R.; Nicholson, J.W.; Swann, W.C.; Coddington, I.; Newbury, N.R. High-Performance, Vibration-Immune, Fiber-Laser Frequency Comb. *Opt. Lett.* **2009**, *34*, 638. [CrossRef]
48. Wu, S.; Morse, T.F.; Strait, J.; Fork, R.L. High-Power Passively Mode-Locked Er-Doped Fiber Laser with a Nonlinear Optical Loop Mirror. *Opt. Lett.* **1993**, *18*, 1444. [CrossRef]
49. Haus, H. Mode-locking of lasers. *IEEE J. Sel. Top. Quantum Electron.* **2000**, *6*, 1173–1185. [CrossRef]
50. Duan, D.; Wang, J.; Wu, Y.; Ma, J.; Mao, Q. Approach to High Pulse Energy Emission of the Self-Starting Mode-Locked Figure-9 Fiber Laser. *Opt. Express* **2020**, *28*, 33603–33613. [CrossRef]
51. Jiang, T.; Cui, Y.; Lu, P.; Li, C.; Wang, A.; Zhang, Z. All PM Fiber Laser Mode Locked With a Compact Phase Biased Amplifier Loop Mirror. *IEEE Photon. Technol. Lett.* **2016**, *28*, 1786–1789. [CrossRef]
52. Pi, Y.; Tian, H.; Li, R.; Han, Y.; Song, Y.; Hu, M. Timing Jitter and Intensity Noise Characterization of a 122-MHz All-PM NALM Mode-Locked Fiber Laser. *IEEE Photon. Technol. Lett.* **2021**, *33*, 1439–1442. [CrossRef]